Nanozyme-Catalyzed Cascade Reaction Enables Highly Sensitive Detection of Live Bacteria

Xuewei Liao,[a,b] Wenjun Tong,[b] Li Dai,[a] Lingfei Han,[a] Hanjun Sun,[b] Wenyuan Liu,*[a] Chen Wang*[b]

[a] College of Pharmacy, China Pharmaceutical University, Nanjing 211198, China

[b] College of Chemistry and Materials Science, Analytical & Testing Center, Nanjing Normal University, Nanjing 210023, China

Corresponding E-mail: liuwenyuan@cpu.edu.cn; wangchen@njnu.edu.cn

Contents

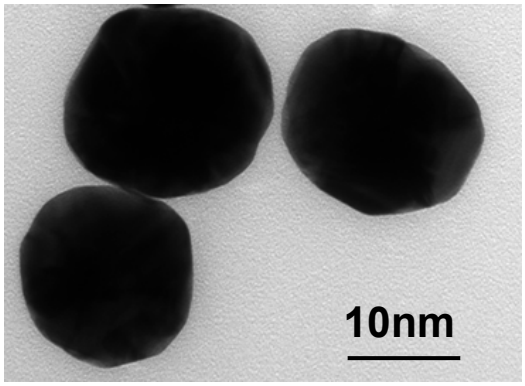

Figure S1. TEM images of AuNPs.

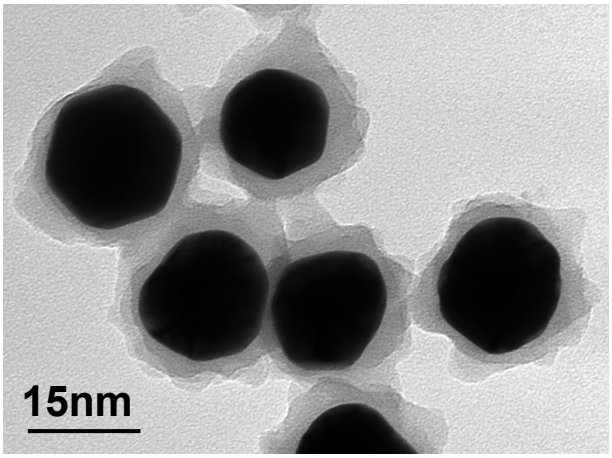

Figure S2. TEM images of Au@POM NPs with 120 min light illumination.

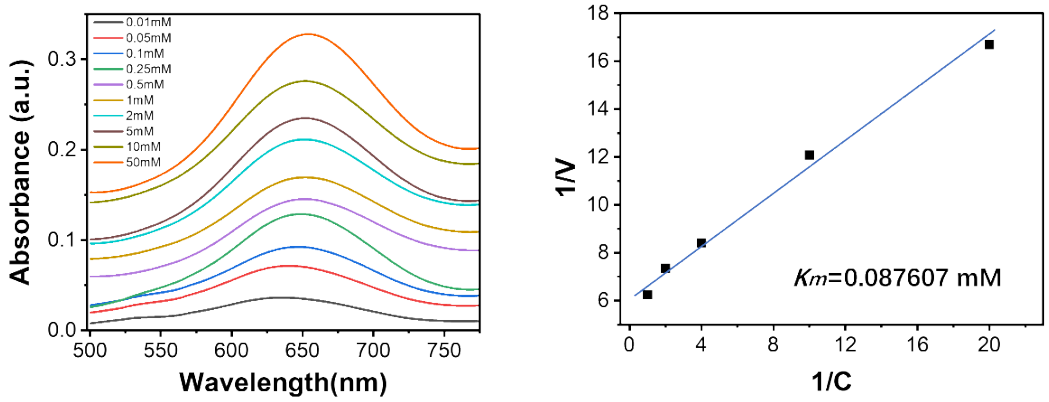

Figure S3. Visible absorbance spectra of AuNPs catalyzed reaction with GOx-like activity and the corresponding double reciprocal plots of nanozyme reaction.

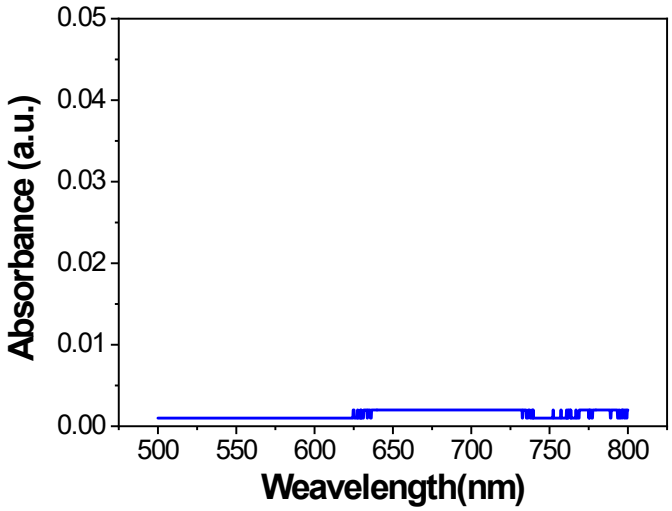

Figure S4. Visible absorbance spectra of the reaction system of POMs + Glucose.

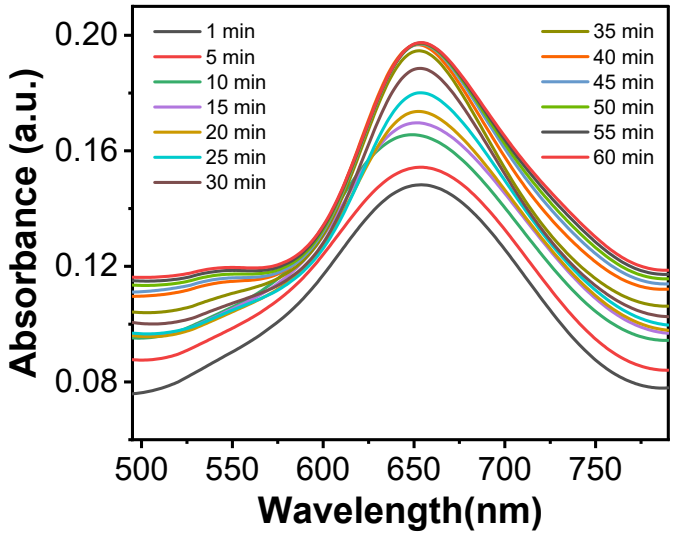

Figure S5. Visible absorbance spectra of the cascade reaction systems with varied reaction time.

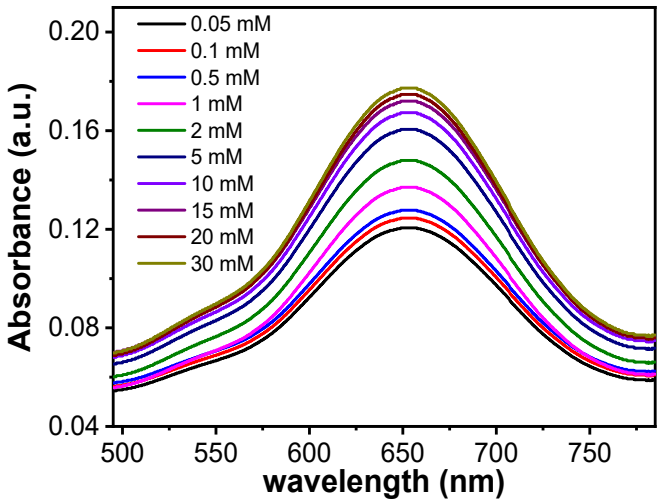

Figure S6. Visible absorbance spectra of the cascade reaction systems with varied glucose concentration.

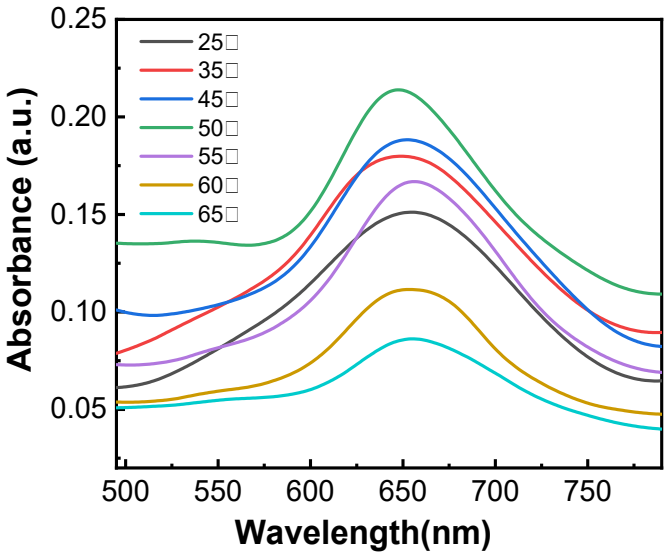

Figure S7. Effect of temperature on the nanozyme activity.

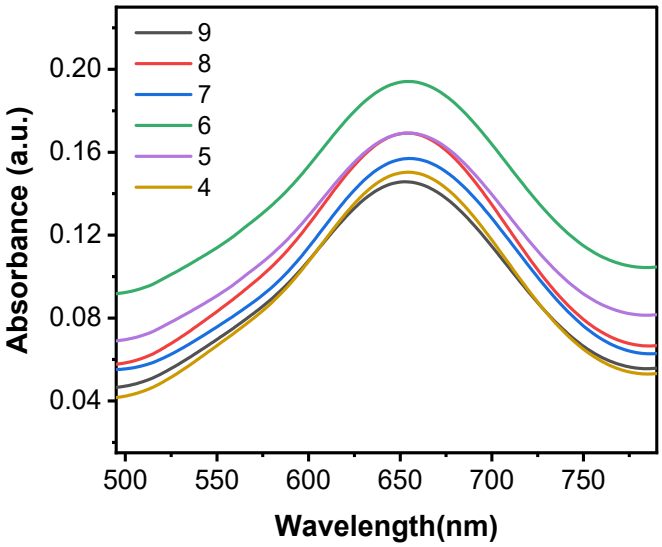

Figure S8. Visible absorbance spectra of the cascade reaction systems under pH values.

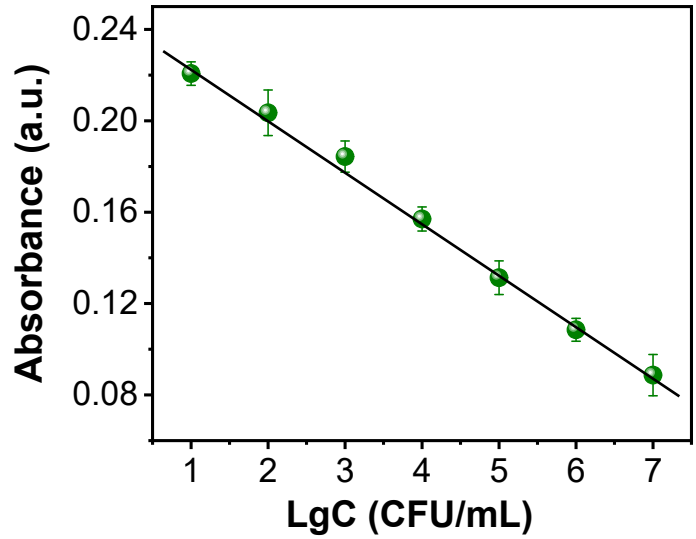

Figure S9. The standard curve of peak absorbance intensity at 625 nm versus the concentation of *S. aureus* bacterium.

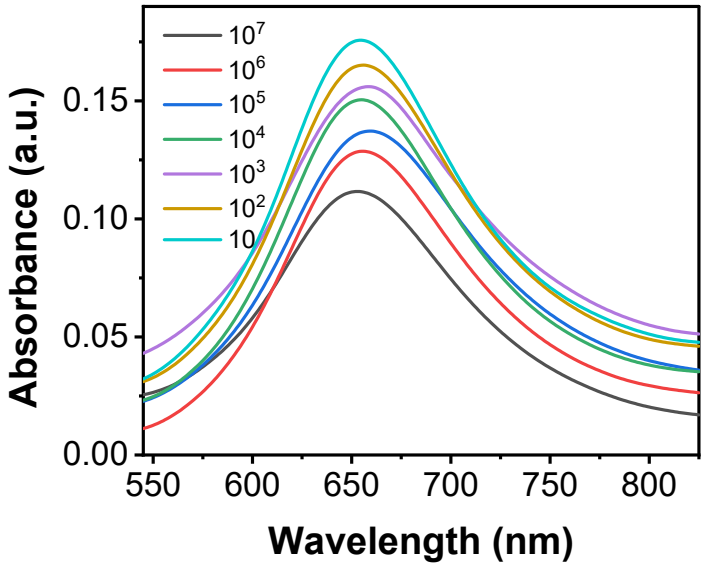

Figure S10. Visible absorbance spectra of the system after addition of different content of *E. coli* bacteria.

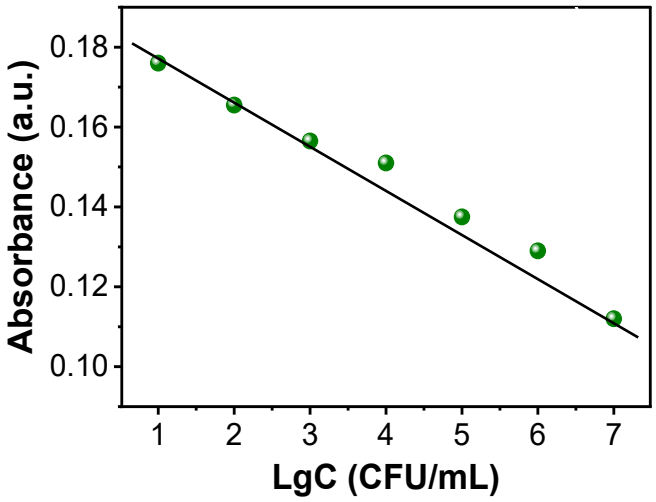

Figure S11. The standard curve of peak absorbance intensity at 625 nm versus the concentation of *E. coli* bacterium.

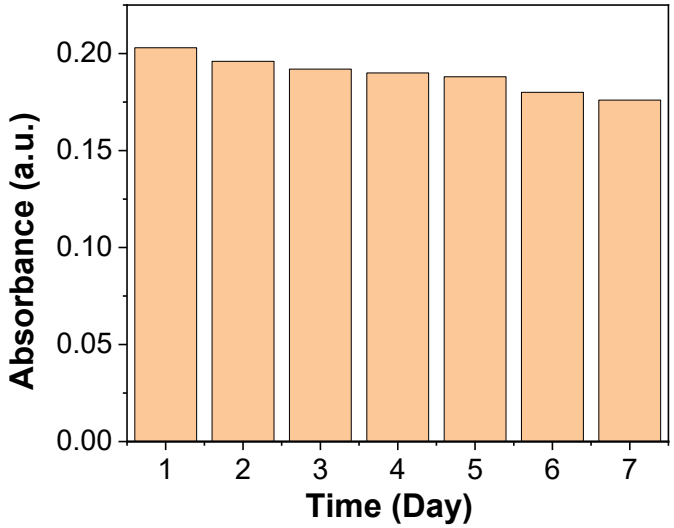

Figure S12. The stability of the present sensor towards glucose detection.

Table S1. Comparison of the performance of different biosensors for bacterial detection.

Detection Technique	Linear range (CFU/mL)	Detection limit (CFU/mL)	Reference
Fluorescent	1.0×10^3 - 1.0×10^9	2.9×10^2	S1
Fluorescent	50 - 10^7	8	S2
Flow cytometry	3.3×10^1 - 3.3×10^5	33	S3
Flow cytometry	1.5×10^2 - 1.5×10^6	40	S4
Colorimetric	10^2 - 10^7	24	S5
Colorimetric	10^2 - 10^7	85	S6
SERS	10^2 - 10^7	35	S7
Microfluidic	500 - 5.0×10^4	50	S8
Electrochemical	10^3 - 10^5	845	S9
Electrochemical	10 - 10^7	13	S10
Digital reading	10^5-10^8	10^4	S11
Nanozyme	100 - 1.0×10^5	22	S12
Nanozyme	5 - 1.0×10^7	5	This work

SERS: Surface-Enhanced Raman Scattering.

Reference

S1. Kong, W. J.; Xiong, J.; Yue, H.; Fu, Z. F. *Anal. Chem.* **2015,** *87* (19), 9864-9868.

S2. Cui, F. C.; Sun, J. D.; Habimana, J. D.; Yang, X. X.; Ji, J.; Zhang, Y. Z.; Lei, H. T.; Li, Z. J.; Zheng, J. Y.; Fan, M. H.; Sun, X. L. *Anal. Chem.* **2019,** *91* (22), 14681-14690.

S3. Meng, X. Y.; Yang, G. T.; Li, F. L.; Liang, T. B.; Lai, W. H.; Xu, H. Y. *ACS Appl. Mater. Interfaces.* **2017,** *9* (25), 21464-21472.

S4. Wang, Y. R.; He, Y.; Bhattacharyya, S.; Lu, S. G.; Fu, Z. F. *Anal. Chem.* **2020,** *92* (4), 3340-3345.

S5. Li, D. K.; Fang, Y. S.; Zhang, X. M. *ACS Appl. Mater. Interfaces.* **2020,** *12* (8), 8989-8999.

S6. Yu, T.; Xu, H.; Zhao, Y.; Han, Y.; Zhang, Y.; Zhang, J.; Xu, C.; Wang, W.; Guo, Q.; Ge, J. *Scientific Reports.* **2020,** *10* (1).

S7. Zhang, H.; Ma, X. Y.; Liu, Y.; Duan, N.; Wu, S. J.; Wang, Z. P.; Xu, B. C. *Biosens. Bioelectron.* **2015,** *74*, 872-877.

S8. Zheng, L.Y.; Cai, G.Z.; Wang, S.Y.; Liao, M.; Li, Y. B.; Lin, J. H. *Biosens. Bioelectron.* **2019**, *124*, 143-149.

S9. Nemr, C. R.; Smith, S. J.; Liu, W. H.; Mepham, A. H.; Mohamadi, R. M.; Labib, M.; Kelley, S. O. *Anal. Chem.* **2019,** *91*, 2847-2853.

S10. Bhardwaj, J.; Devarakonda, S.; Kumar, S.; Jang, J. *Sens. Actuator B-Chem.* **2017,** *253*, 115-123.

S11. Huang, H. R.; Zhao, G.Y.; Dou, W. C. *Biosens. Bioelectron.* **2018**, *107*, 266–271.

S12. Zhou, J.; Tian, F. Y.; Fu, R. J.; Yang, Y. J.; Jiao, B. N.; He, Y. *ACS Appl. Nano*

Mater. **2020**, *3*, 9016-9025.